Available online at www.sciencedirect.com
SCIENCE DIRECT®
Journal of the European Ceramic Society 25 (2005) 2471–2475
www.elsevier.com/locate/jeurceramsoc

A new family of ferroelectric tetragonal tungsten bronze phases, $Ba_2MTi_2X_3O_{15}$

M.C. Stennett, G.C. Miles, J. Sharman, I.M. Reaney, A.R. West

Department of Engineering Materials, The University of Sheffield, Sir Robert Hadfield Building, Mappin Street, Sheffield S1 3JD, UK

Available online 20 April 2005

Abstract

The compositions $Ba_2MTi_2X_3O_{15}$: M = La, Pr, Nd, Sm, Eu, Gd, Dy, Bi; X = Nb, Ta form a new family of ferroelectric phases. With larger M cations, La, Bi, the materials exhibit relaxor behaviour with sub-ambient Tc. With decreasing M size, a sharp first order ferroelectric phase transition is observed and Tc rises to a maximum at ∼330 °C for Gd. The phases are tetragonal tungsten bronzes with A-site order (BaM) and non-statistical B-site disorder (of Ti, Nb for M = La). All phases show a weak superstructure with doubled *c* and multiple periodicity parallel to [1 1 0] that is incommensurate for the relaxor ferroelectrics (M = La, Bi) but commensurate for the remainder. The phases exhibit complex non-stoichiometry with variable Ba:M and Ti:X ratios as well as variable oxygen content.

Keywords: Powders-solid state reaction; Dielectric properties; Ferroelectric properties; Electron microscopy; Neutron diffraction

1. Introduction

A large part of the electroceramics industry is driven by the development of new materials for communications applications. Materials requirements come into three categories: high permittivity, low dielectric loss and low temperature coefficient of permittivity. Chen et al.[1,2] reported high permittivities at microwave frequencies for phases in the system $BaO\text{-}M_2O_3\text{-}TiO_2\text{-}X_2O_5$ (M = rare earth). The properties of a number of compositions were reported, but the stoichiometry of the single phase compositions and the dependence of properties on stoichiometry and crystal chemistry were uncertain. We embarked on a study of these materials to clarify their stoichiometry, structure and properties and summarise here developments to date.

Compositions $Ba_2MTi_2Nb_3O_{15}$ (M = Bi, La, Pr, Nd, Sm, Eu, Gd, Dy) were produced by a conventional mixed-oxide processing route. To determine the reaction temperature, for each composition, 0.5 g batches were ground and mixed in a pestle and mortar, placed in a platinum crucible, and reacted at temperatures in the range 1200–1350 °C for 2 h. Following each reaction the powders were checked for phase purity using a Philips Hagg–Guinier camera (Eindhoven, Holland). This process was repeated until the compositions were single-phase by XRD. Using the information from this initial trial, large 100 g batches were then prepared.

The powder precursors were weighed out and attrition milled, using a Szegvari Attritor System Model 01-HD supplied by Union Process (Akron, USA), in a 750 ml mill pot (Tefzel-coated stainless steel) containing 1500 g of partially stabilised (Y_2O_3) zirconia media (3 mm) and 200 ml of *iso*-propanol. A rotation speed of 300 rpm was employed for 1 h to ensure a homogeneous distribution of all the reactants throughout the batch and reduce the powder particle size to ∼1 μm. The slurry was separated from the media using a sieve, dried overnight at 100 °C, then sieved further using a 200 μm mesh.

The mixed powder batches were reacted for 8 h in an open alumina crucible in air. The products were then attrition-milled for 1 h, to break up the agglomerates formed during reaction. This milling step was identical to that used to reduce the raw material particle size except that after 45 min, 2 wt% polyethylene glycol (PEG) binder was added to the slurry. 20 mm diameter pellets were pressed in a hardened stainless steel die (∼6 g of powder) at ∼30 MPa. The pellets were sintered between 1100 and 1450 °C, depending on

E-mail address: a.r.west@sheffield.ac.uk (A.R. West).

0955-2219/$ – see front matter © 2005 Elsevier Ltd. All rights reserved.
doi:10.1016/j.jeurceramsoc.2005.03.198

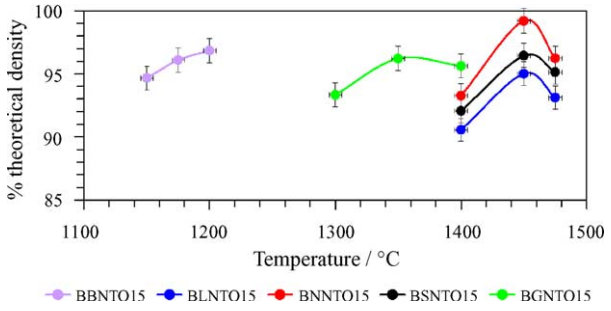

Fig. 1. Percentage theoretical density of the $Ba_2MTi_2Nb_3O_{15}$ (M = Bi, La, Nd, Sm, Gd) compositions as a function of sintering temperature.

composition, for 4 h in air on a zirconia tile (3 °C min^{-1} ramp rate). The optimum sintering temperature was determined so as to achieve the maximum pellet density, Fig. 1. Maximum densities were usually obtained close to the melting temperature. In the case of La-, Nd- and Sm-analogues, optimum density was achieved at 1450 °C; when heated to 1475 °C, pellets showed no signs of deformation but density had decreased due to de-sintering associated with grain growth.

A rough density of each pellet was established via the Archimedes method using the equation:

$$\rho_{\text{pellet}} = \frac{m_0}{[(m_0 - m_1) + (m_2 - m_0)]/\rho_{\text{water}}}$$

To calculate the density, three weights were required, m_0, the dry weight, m_1, the immersed weight and m_2, the soaked weight. The difference between m_0 and m_1 is the mass of water displaced by the ceramic. Assuming the immersion liquid fills all the open porosity in the ceramic, $(m_0 - m_1)/\rho_{\text{water}}$ is equivalent to the volume of the ceramic and the closed porosity. The difference between m_2 and m_0 is the mass of the water that has filled the open porosity in the ceramic which can also be converted into a volume, the volume of the open porosity. Hence

$$\rho_{\text{pellet}} = \frac{m_0}{V_{\text{pellet}}}$$

The relative densities were calculated by comparison with the theoretical X-ray powder densities.

All microstructural characterisation was carried out on fracture surfaces thermally-etched at 90% of the optimum sintering temperature. The microstructures of the Bi-, La- and Sm-compositions consisted of needle-like grains approximately 1–10 μm in length and 1–3 μm in width. The microstructures of the Gd- and Nd-analogues were composed of more equiaxed grains, approximately 1–8 μm in diameter. There was no indication of exaggerated grain growth in any of the samples examined and they all exhibited few pores with a density >95% of the theoretical value. Fig. 2 shows the microstructures of the $Ba_2LaTi_2Nb_3O_{15}$ and $Ba_2NdTi_2Nb_3O_{15}$ compositions.

Initial phase diagram studies on the system BaO-La_2O_3-TiO_2-Nb_2O_5 showed the existence of a solid solution phase belonging to the tetragonal tungsten bronze family. Its complete stoichiometry range has still not been determined but it is clear that it has variable Ba:La and Ti:Nb ratios and the oxygen content is also variable. In seeking an 'ideal' composition for the 'parent' phase, on which the solid solutions may be based and described, the composition $Ba_2LaTi_2Nb_3O_{15}$ appeared to be a clear possibility[3]; subsequent studies have shown that a number of analogues, containing a large rare earth cation or Bi^{3+} instead of La, and either Nb or Ta, can be prepared.[4] X-ray powder diffraction, XRD, data were indexed on primitive tetragonal unit cells with $a \sim 12.43$, $c \sim 3.93$ Å; a increases gradually with rare earth size, whereas c is almost independent of composition.[4]

The crystal structure of $Ba_2LaTi_2Nb_3O_{15}$ was determined using a combination of XRD and variable temperature powder neutron diffraction, ND data.[5] ND data were recorded

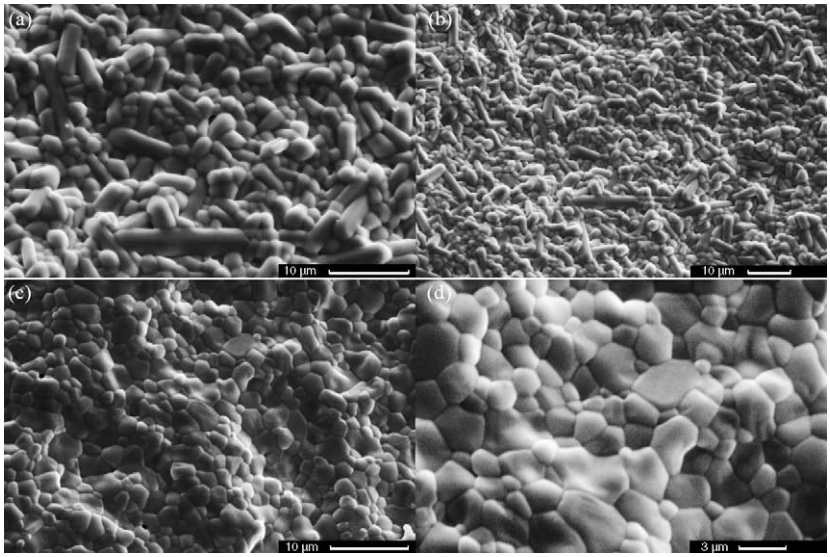

Fig. 2. SEM micrographs of (a and b) $Ba_2LaTi_2Nb_3O_{15}$ and (c and d) $Ba_2NdTi_2Nb_3O_{15}$.

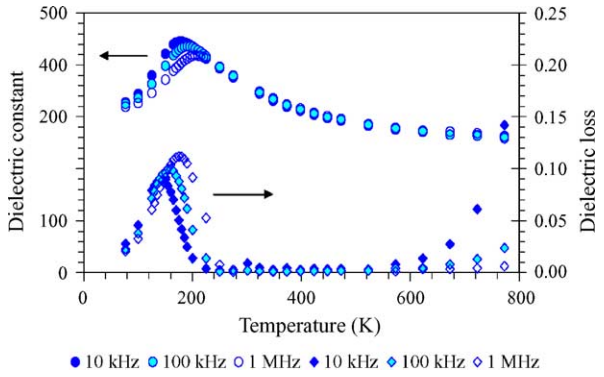

Fig. 3. Dielectric constant (permittivity) and dielectric loss as a function of temperature for composition $Ba_2LaTi_2Nb_3O_{15}$.

at 100 and 400 K, to either side of the relaxor ferroelectric to paraelectric phase transition, whose temperature is frequency-dependent, in the range 170–200 K, Fig. 3.[3] Both structures belong to the general tetragonal tungsten bronze, TTB, family, Fig. 4, with Ba and La fully ordered on the large 15- and 12-coordinate sites, respectively. Nb and Ti are disordered over the octahedral sites, but the distribution is non-statistical, with a slight preference of Nb for site (2) and conversely, of Ti for site (1).[5]

At 100 K, the structure has the non-centrosymmetric space group *P4bm*, which allows Ti and/or Nb to undergo small, off-centre displacements within the (Nb/Ti)O_6 octahedra, leading to a polar *c* axis. At 400 K, the structure is centrosymmetric, space group *P4/mbm* and there is little evidence of polarity within the largely undistorted (Nb/Ti)O_6 octahedra.

These structural studies clearly showed the origin of the low temperature ferroelectric behaviour to be associated with displacements of Nb/Ti within their octahedra; what is still not clear is why this material should show relaxor behaviour; possibly, the polarisation within the two sets of (Nb/Ti)O_6 octahedra commences at different temperatures; alternatively, perhaps individual NbO_6 and TiO_6 octahedra exhibit different temperature-dependence in their polarisation; either effect could contribute to relaxor behaviour in which the phase transition is spread over a range of temperatures.

The structures determined by ND do not give a complete description since selected area electron diffraction, SAD, on small single crystal grains of $Ba_2LaTi_2Nb_3O_{15}$ showed the presence of additional diffraction effects leading to a superlattice, Fig. 5.[5,6] Additional rows of weak spots are seen, consistent with a doubling of the *c* axis. However, the superlattice is also present in the [1 1 0] direction, but its periodicity is incommensurate with that of the sublattice.[5]

More recent studies on other M analogues[6] show that all possess a superlattice with a doubling of *c*; however, the periodicity parallel to [1 1 0] is incommensurate for M = La, Bi but commensurate for smaller rare earths, e.g. Nd, Sm, Gd. The structural origin of the superlattice and the effect, if any, on the properties is not known at present. It is probably

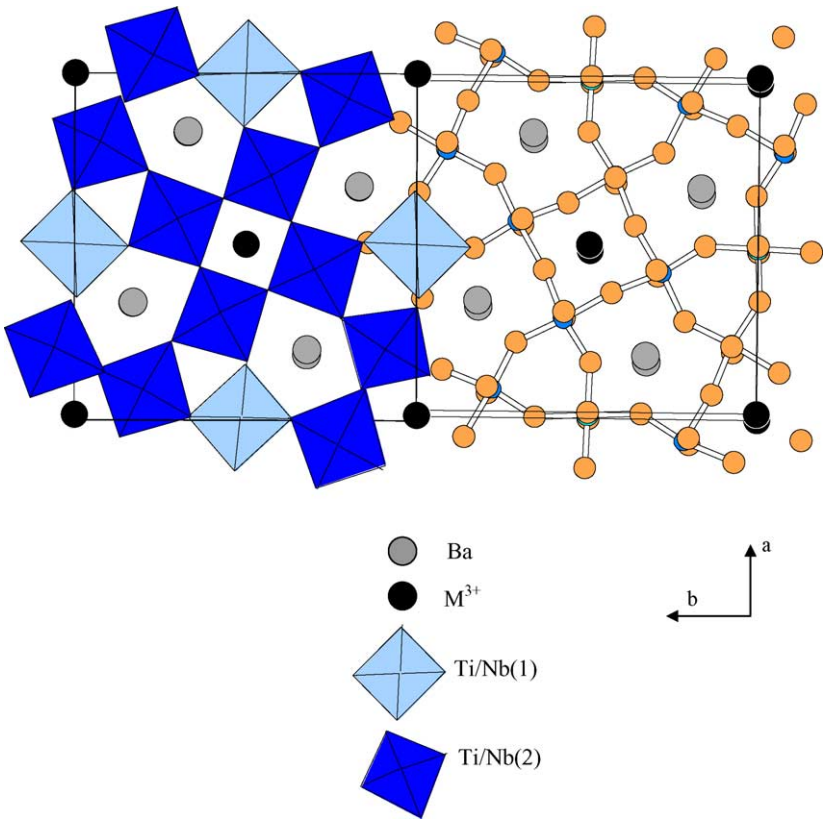

Fig. 4. *ab* Projection of the TTB crystal structure. Two unit cells are shown; the (Ti, Nb)O_6 octahedra (left) and the (Ti, Nb)–O bonds (right) are highlighted.

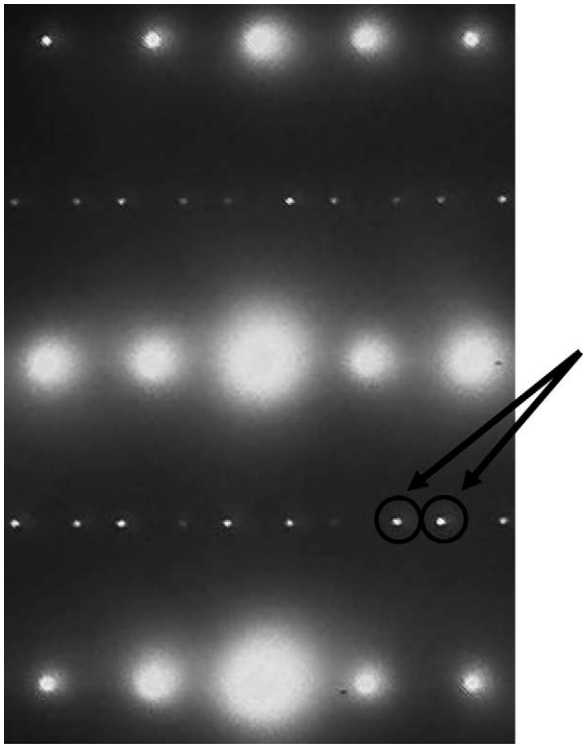

Fig. 5. [1 1 4] Zone axis electron diffraction pattern for $Ba_2LaTi_2Nb_3O_{15}$. The additional incommensurate superlattice reflections are highlighted.

not coincidental that the two phases that exhibit relaxor behaviour [M = La, Bi] are also those where the superlattice is incommensurate parallel to [1 1 0]. Nevertheless, it is intriguing that these commensurate/incommensurate superlattice effects should occur in the *ab* plane whereas the structural refinements indicate that *c* is the polar axis in the ferroelectric state.

For the family of phases, $Ba_2MTi_2Nb_3O_{15}$, the Curie temperature increases with decreasing M size, from ~200 K for M = La and Bi to ~600 K for M = Gd, Fig. 6.[6] At present, we cannot comment on any variation of the permittivity, ε'_{max}, at Tc with M size. There is clear evidence that the permittivity-temperature profile depends on sample processing conditions, and our data are probably not optimised; however, for a given composition, Tc does not vary, as shown for data on the M = Gd analogue, Fig. 7.

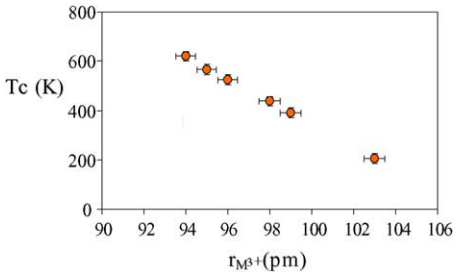

Fig. 6. Temperature at the permittivity maximum, Tc, vs. ionic radius of M.

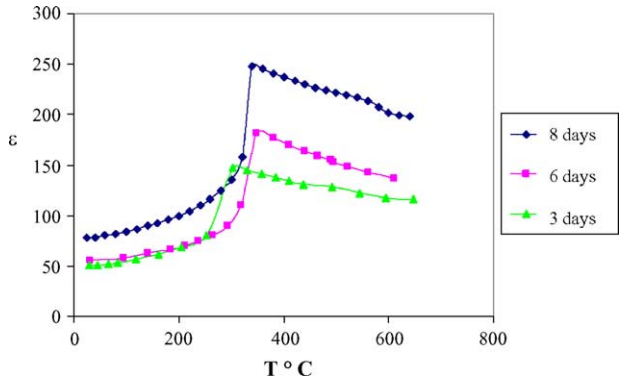

Fig. 7. Permittivity data for composition $Ba_2GdTi_2Nb_3O_{15}$, at 1250 °C showing an increase in permittivity with increased heating times during solid state synthesis

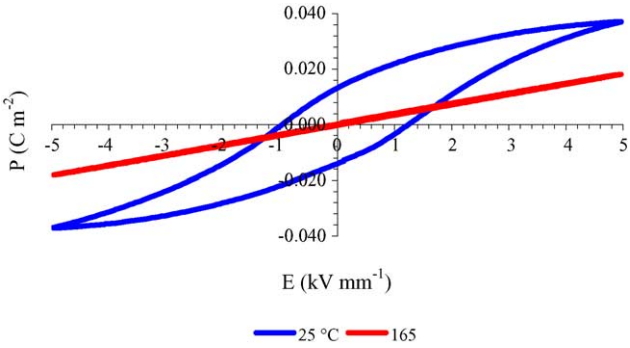

Fig. 8. Hysteresis curves for composition $Ba_2NdTi_2Nb_3O_{15}$. Ferroelectric behaviour is exhibited at room temperature but not at 165 °C, which is above Tc.

Confirmation of the ferroelectric–paraelectric nature of the phase transition at Tc has been shown by hysteresis loop data for three compositions at two temperatures. Profiles for the Nd-analogue are given in Fig. 8. The data recorded at 25 °C were obtained from the ferroelectric phase and consequently exhibit typical hysteresis loop behaviour. The data obtained at 165 °C reflect the behaviour of a paraelectric phase and consequently, no hysteresis loop is observed.

Acknowledgements

We thank the EPSRC and Filtronic Comtek for financial support and Dr. David Hall at the University of Manchester for help with the high field dielectric measurements.

References

1. Chen, X. M. and Yang, J. S., Dielectric characteristics of ceramics in the BaO-Nd_2O_3-TiO_2-Ta_2O_5 system. *J. Eur. Ceram. Soc.*, 1999, **19**, 139–142.
2. Chen, X. M., Liu, C. L., Yang, J. S. and Wu, Y. J., Dielectric ceramics modified by Bi substitution for Nd. *J. Solid State Chem.*, 1999, **148**, 438–441.

3. Kirk, C. A., Stennett, M. C., Reaney, I. M. and West, A. R., A new relaxor ferroelectric. *J. Mater. Chem.*, 2002, **12**, 2609–2611.
4. Miles, G. C., Stennett, M. C., Pickthall, D., Kirk, C. A., Reaney, I. M. and West, A. R., X-ray diffraction data for the new ferroelectric tetragonal tungsten bronze phases, $Ba_2RETi_2M_3O_{15}$: M = Nb and RE = La, Pr, Nd, Sm, Eu, Gd, Dy, (Bi); M = Ta and RE = La. *Nd. Powder Diffraction*, 2005, **20**(1), 43–46.
5. Miles, G. C., Stennett, M. C., Reaney, I. M. and West, A. R., Temperature dependent crystal structure of ferroelectric $Ba_2LaTi_2Nb_3O_{15}$. *J. Mater. Chem.*, 2005, **15**, 798–802.
6. Stennett, M. C., Reaney, I. M., Levin, I., Miles, G. C., Woodward, D. I., Kamba, S. *et al.*, Dielectric and structural studies of $Ba_2ReTi_2Nb_3O_{15}$ Re = Bi, La, Nd, Sm, Gd) tetragonal tungsten bronze-structured ceramics. *J. Am. Ceram. Soc.*, in preparation.